Jurnal Teknik Mesin
Mechanical Xplore (JTMMX)
Mechanical Engineering
Vol. 5 No. 1 (2024) pp. 24-37
p-ISSN: 2746-0045 e-ISSN: 2746-3672

Progressive Dies for L-hanger Ducting (L-HD) Utilizing Low-Carbon Steel SPCC-SD Material: An Experimental and Numerical Analysis

Ade Cepi Budiansyah[1], Muhamad Taufik Ulhakim[1*] Sukarman[1], Agus Supriyanto[1], Amir[1], Dodi Mulyadi[1], Khoirudin[2]

[1]Department of Mechanical Engineering, Faculty of Engineering, Universitas Buana Perjuangan Karawang, Karawang, 41361, West Java, Indonesia.

[2]Department of Mechanical Engineering, Faculty of Engineering, Universitas Sebelas Maret, Surakarta, 57126, Central Java, Indonesia.

ABSTRACT

Industrial development in manufacturing and construction has highlighted L-Hanger Ducting as a key component in HVAC systems, providing support and stabilization for air ducts. The manufacturing process of L-Hanger Ducting includes blanking, piercing, and bending stages. This research focuses on designing and simulating punches for these processes using 1.6 mm thick SPCC-SD material. The objectives are to design and analyze progressive dies to improve production efficiency and to predict the tonnage requirements of the press machine. A multi-methodological approach was used, integrating mathematical analysis, numerical analysis, and experimental validation. Mathematical analysis calculated the overall forces, which were compared with numerical results and verified experimentally. The smallest maximum punch length calculated was 47.16 mm. Theoretical deflection values for punch piercing 1-3 were 0.03 mm, 0.07 mm, and 0.06 mm, while simulation results showed deflections of 0.03 mm, 0.05 mm, and 0.06 mm. The maximum von Mises stress in piercing 1-3 from simulations was 205.6 N/mm², 439.4 N/mm², and 568.5 N/mm², below the yield strength of SKD 11 JIS G4404 material at 2970 N/mm². By optimizing the design of progressive dies, it is expected that the production efficiency of L-Hanger Ducting will increase, expanding knowledge in metal forming and contributing to advancements in the metal forming industry and scientific development.

Keywords: *Heating ventilation and air conditioning,* L-hanger ducting, *Progressive dies, Metal forming, Force bending*

Article information:
Submitted: 09/07/2024
Revised: 04/09/2024
Accepted: 06/09/2024

Author correspondence:

* ✉: muhamad.ulhakim@ubpkarawang.ac.id

Type of article:

☑ Research papers

☐ Review papers

1. INTRODUCTIONS

The manufacturing industry's evolution requires constant innovation in production processes to improve efficiency and product quality. One of the main obstacles in producing metal goods like L-Hanger Ducting (L-HD) is dealing with the springback phenomenon that occurs during the forming process. Previous research has demonstrated that utilizing specific materials, such as 1.6 mm-thick SPCC-SD, necessitates a meticulous design approach when employing progressive dies to create accurate geometries. This inquiry explores the design details and assesses the effectiveness of progressive dies designed for L-HD items made from SPCC-SD 1.6 mm material. This study aims to improve the efficiency and production quality process

DOI: 10.36805/jtmmx.v%vi%i.7763

for complex metal products like L-HD by thoroughly studying the metal-forming process and material properties. Further study is necessary to design and use optimum progressive dies in the L-HD production process.

The introduction to plate bending processes emphasizes three primary forming methods: air bending, wipe-die bending, and V-die bending [1-5]. Air bending, known for its flexibility, is widely preferred in sheet metal bending. Gupta and H. S. Payal [6] delve into its effects on the spring-back phenomenon in electro-galvanized CR4 steel and investigate die-making for Isuzu Traga vehicles conducted by [7]. Designing die compounds for TVS-N54-type cylinder head gaskets is a pivotal study to enhance forming precision and efficiency [8]. Further research on determining the minimum empty seat gap, experimenting with drawing in rectangular cups [9]. experimenting with drawing rectangular cups, and leveraging SOLIDWORKS software for progressive mold design propel advancements in metal-forming technology. These efforts signify diverse endeavors toward process optimization and heightened efficiency in metal-forming industries [10]. Tikamori et al. [7], conducted finite element of round cup deep drawing as provided in **Figure 1**.

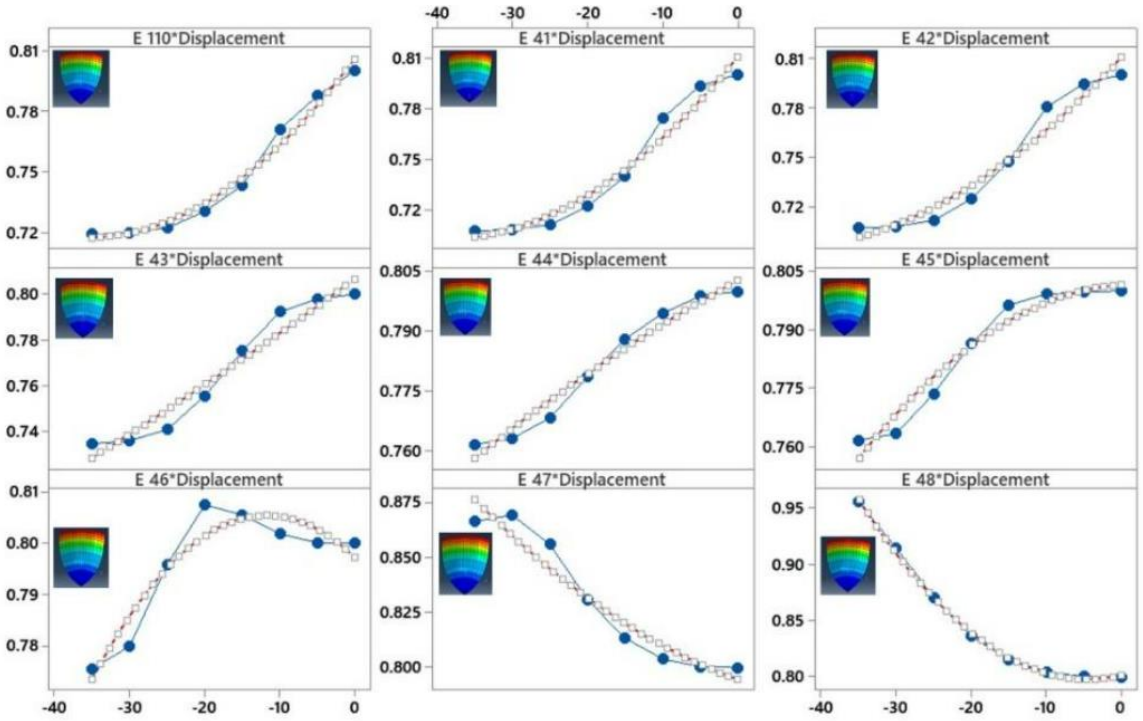

Figure 1. Finite element of round cup deep drawing simulatied by Tikamori et al [7]

Previous research has extensively explored advancements in bending processes, as evidenced by several studies. S. Chatti et al. [11] introduced a method enabling the three-dimensional bending of profiles with diverse cross-sections in the TSS bending process. Meanwhile, M. F. Adnan et al. [12] utilized the Taguchi Method to analyze spring-back behavior in AA6061 materials with non-uniform thickness. G. M. S. Ahmed et al. [13] conducted experimental evaluations of spring-back in mild steel, validated through LS-DYNA simulations. J. R. Cho and S. J. Moon et al. employed the finite element method to analyze spring-back properties in U-bending sheet metal processes. Ouakdi et al. [14] delved into spring-back evaluation considering holding force, dead radius, and material properties. These studies collectively address

knowledge gaps and resolve spring-back concerns in metalworking processes—research into spring back in vee bending processes for high-strength materials was conducted by [4]. The investigations enhancing manufacturing support through process analysis further contribute to understanding and improving bending processes reported by [15]. A. Adelkhani et al. [16] exploring welding angle effects on multi-layered sheet formation during U-bending and A. Badrish et al. [17] aimed to reduce spring-back in Inconel 625 alloy during thermomechanical V-bending. M. Özdemir et al. [18] utilized numerical modelling to investigate spring back and bending synchronization in Cr-Mo alloyed sheet materials, while R. Srinivasan et al.[19] utilized numerical modeling to investigate spring-back and bending synchronization in Cr-Mo alloyed sheet materials, while R. Thipprakmas et al. [20] introduced the spring-back factor in V-bending die design, enhancing precision. S. Thipprakmas and W. Phanitwong [21] used the Taguchi method to reduce spring-back effects in V-bending. M. A. Wahed [22] optimized parameters for Ti-6Al-4V alloy to reduce spring-back. H. Y. Yu [23] explored the effects of modulus of elasticity changes on spring-back and solidification in plastics, while J. Zhang et al. [24] investigated carbon steel spring-back in die forming processes. These studies collectively advance understanding and techniques for managing spring-back phenomena across various materials and bending processes.

This study focuses on the manufacturing process of L-Hanger Ducting (L-HD), involving piercing, blanking, and bending of 1.6 mm SPCC-SD material. It addresses the challenge of spring-back phenomena inherent in this material by introducing innovative concepts for designing and evaluating progressive dies tailored to specific product shapes, including an analysis of the L-HD product itself. The research explores effective strategies for mitigating springback through design adaptations and specialized bending techniques. Additionally, it provides practical insights into die design and spring-back mitigation for materials with unique properties, advancing our understanding of advanced mold design for L-HD products. The study also investigates variations in elastic modulus during plastic deformation, a critical factor in developing advanced dies and punches suitable for goods made from 1.6 mm SPCC-SD material. Ultimately, this project aims to fill knowledge gaps by developing new die designs specifically tailored for 1.6 mm SPCC-SD material and the distinct shape of L-HD products.

2. Materials and Methods

2.1. Material

The material used in fabricating L-HD products is a 1.6 mm-thick cold-rolled steel plate from SPCC type SD. SPCC Cold Rolled Steel meets commercial quality standards defined in JIS G 3141 [25-27]. According to this standard, SPCC-SD contains up to 0.12% carbon (C), up to 0.5% manganese (Mn), up to 0.04% phosphorus (P), and up to 0.045% sulfur (S). The mechanical properties of SPCC-SD (JIS G3141) are comprehensively detailed in **Table 1**.

Table 1. The mechanical properties of SPCC-SD and SKD 11

Specification	Yield strength (MPa)	Tensile strength (MPa)	Elongation (%)	Reff.
JIS G 3141-SPCC-SD	≤240	≥270	≥46	[28]
JIS G 4404-SKD 11	2970	370	56	[29]

Punches and dies are crucial for forming and cutting operations. These tools require specific characteristics such as high compressive strength and the ability to harden up to 60 HRC [30]. Therefore, SKD 11 has been chosen as the material for these tools. SKD 11 is an alloy steel known for its high levels

DOI: 10.36805/jtmmx.v%vi%i.7763

of carbon and chromium, resulting in significant hardness and wear resistance after heat treatment. It exhibits excellent hardening resistance and dimensional stability. According to the JIS G4401 standard, the chemical composition of SKD 11 includes carbon (C) ranging from 1.40% to 1.60%, silicon (Si) up to 0.30%, manganese (Mn) up to 0.60%, phosphorus (P) up to 0.030%, sulfur (S) up to 0.030%, chromium (Cr) from 11% to 13%, vanadium (V) up to 0.50%, and molybdenum (Mo). The mechanical properties of SKD 11 (JIS G4404) can be found in **Table 1**.

2.2. Progressives dies and layout strip

This study utilized the SolidWorks Student Version to simulate progressive dies. The research aims to determine various characteristics of press tools relevant to the blanking process: material composition, dimensions, cutting and bending forces, forming effort, and clearance. Subsequently, Abaqus Student Version software was employed for simulation. The progressive die design was developed using established formulas for total punch piercing and bending. The total punch tonnage was then used to assess the press machine's capacity.

L-Hanger Ducting (L-HD) products are manufactured from SPCC-type SD steel plates, cold-rolled to a thickness of 1.6 mm. Strip layouts were adjusted according to the material thickness. With a material thickness (t) of 1.6 mm, the B value was calculated as 1.5 x 1.6 = 2.4 mm. Adding 17 mm to twice the B value results in the W value, calculated as 17 + (2 x 2.4) = 21.8 mm.

The L-HD manufacturing process involves five stages: three piercing stages (piercing 1-3), one bending stage, and one blanking stage. The process begins with oblong piercing, progresses through hole piercing, and concludes with piercing 3. The fourth stage involves bending and blanking to complete the product formation. **Figure 2** illustrates the progressive dies, strip layout, blank dimensions, and the final L-HD product.

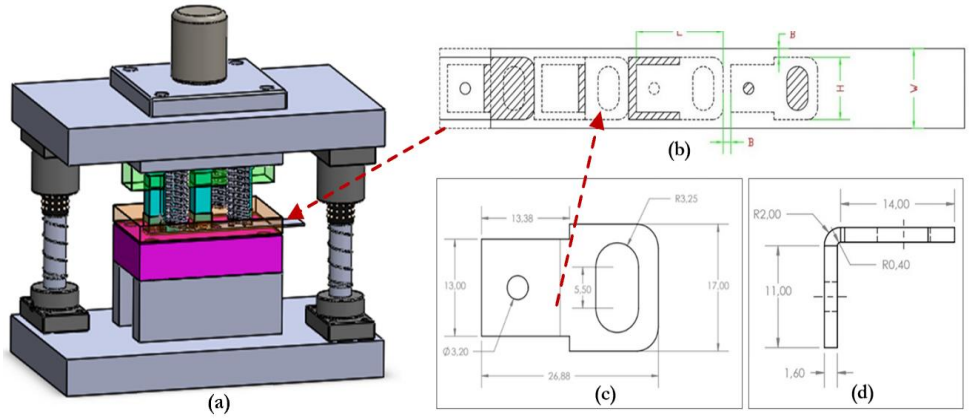

Figure 2. Dies L-HD product-all dimension in mm: (a) Dies assembly (b) Layout strip, (c) Blank L-HD (d) Bending

2.3. Design for calculation

The calculation of piercing force involves assessing the pressure based on the material's shear stress and yield strength. The piercing force F_p is determined by multiplying the shear stress τ_g the perimeter *l* of the workpiece, and the thickness **s** of the material plate, as shown in Equation (1) [31]:

$$F_p = \tau_g \, x \, l \, x \, s \quad (1)$$

Where F_P represents the piercing force in Newtons, *l* denotes the perimeter of the workpiece (mm), *s* the thickness of the material plate (mm), and τ_g denotes the shear stress of the material (N/mm²). These parameters are essential for analyzing the cutting process and evaluating die performance. The product opening or blank length, as depicted in Figure 1(d) can be determined using Equation [4].

DOI: 10.36805/jtmmx.v%vi%i.7763

$$L = a + b + V \quad (2)$$

Where v is the compensation factor, calculated according to DIN 6935 for opening angles between 0° and 90°, as shown in Equation (3).

$$V = \pi \left(\frac{180^0 - \beta}{180^0}\right) x \left(r + \frac{s}{2} xk\right) - 2(r + s) \quad (3)$$

The correction factor *k* takes values based on for r/s > 5, k = 1, and for r/s < 5, k = 0.65 + (1/2 x log r/s). Subsequently, the bending force requirement, F (N), can be calculated using Equation (4) [4].

$$F = \frac{TS.W.s^2}{D} \quad (4)$$

where TS for tensile strength, w is the width of the product opening (mm), and *s* is the thickness material thickness (mm).

The stripping force is crucial in determining the material blank strip requirement during blanking and piercing. Typically, the stripping force is around 2.5% - 20% of the cutting force, estimated using Equation (5).

$$F_{p_s} = 2{,}5 - 20\% \text{x} F_{p_T} \quad (5)$$

Where, F_{ps} represents the stripper spring force (N), F_{pT} represents the total punch force (N).

The design of dies and the press machine requires matching machine capacity. Equation (6) calculates the press machine capacity (P_m).

$$P_m = (F_s + F_{st}) x\ (S_f) \quad (6)$$

P_m is the press machine capacity (N), F_s is the cutting force (N), S_f is the safety factor ensuring die stability and reliability and F_{st} is the stripping force (N).

Calculating punch length is critical to prevent deflection during cutting, blanking, and bending processes. The maximum punch length, l_{max1} is calculated using Equation (7).

$$l_{max1} = \sqrt{\frac{\pi^2.E.I}{F_p}} \quad (7)$$

Where $I = \frac{\pi.D^4}{64}$ is the moment of inertia (m^4) for the diameter, D. The calculation of maximum punch length (L) is influenced by the elastic modulus (E), which measures how far a material can regain its shape after undergoing elastic deformation. The material inertia moment (I) is a measure of the material's resistance to shape change, including the punch diameter (D) and the force acting on the punch (F_p). The length and width of dies are planned based on the work layout size. The die thickness, h (mm), can be calculated using Equation (8) [4].

$$h = \sqrt[3]{\frac{F_{tot}}{g}} \quad (8)$$

The calculation of the minimum thickness requirement for the striper plate (h) involves three crucial variables: the total force (F_{tot}) measured in Newtons, the gravitational acceleration (g) expressed in meters per second squared, and the dimensions of the product, including its width (w) and the thickness of its material (t). These variables are essential for determining the optimal thickness for the striper plate to function effectively within the press tool system. The calculation, governed by Equation (9), ensures that the striper plate meets the necessary structural requirements and can withstand the forces exerted during the metal-forming process. This analysis is vital for ensuring the press tool components' durability, stability, and performance during operation.

$$h = \frac{1}{3}w + 2s \quad (9)$$

The computation of punch deflection assesses the degree of deformation or bending that arises during its utilization in material cutting or forming operations. This assessment is pivotal in ascertaining the punch's

DOI: 10.36805/jtmmx.v%vi%i.7763

resilience and operational efficacy while ensuring the precision and quality of the outcomes in metal forming processes. Equations (10), (11), and (12) are employed to determine the deflection on punch piercing 1-3, deflection on the die, and deflection on the striper plate.

$$F_P = 0.8 \text{ x } F_p \quad (10)$$

$$\delta = \frac{F_p \text{ .L}}{A_p.E} \quad (11)$$

The cutting force (F_p) is what's needed to cut material, including the actual cutting force (F). Deflection (δ) refers to how much the punch bends during cutting, and the modulus of elasticity (E) measures how well a material bounces back after bending. The cross-sectional area (A) is the material's width, often found using SolidWorks. Punch length (L) is how long the cutting tool is. These factors are crucial for understanding and improving cutting operations. F is the cutting force in Newtons (N), and F_{total} is the total cutting force over the area. Moment of inertia, $\delta = \frac{bh^3}{12}$ in mm^4 is vital for knowing how much the punch bends (δ). Pressure on punch piercing (P_h) 1-3 dies and the striper plate (P_d) can be computed using Equations (12) and (13).

$$P_h = \frac{F}{A} \quad (12)$$

$$P_d = \frac{F_p}{A_d} \quad (13)$$

The factor of safety S_f is calculated using the formula $S_{f1} = \frac{Y_S}{P_{h1}}$ for Piercing 1-3. Safety Factor (Sf) is a crucial parameter that evaluates the safety level of a system or component. It is determined by dividing the material's Yield Strength (Y_s) by the stress applied to the punch (P_h). Yield Strength (Ys) represents the stress threshold where the material undergoes permanent deformation. Stress on the punch (P_h) measures the pressure exerted on the punch during the hole-making process.

3. Result and Discussion

3.1. Analysis of power press tonnage requirements

The analysis method for determining the tonnage requirement of the power press begins with analysing component drawings, studying press parts, and calculating piercing force, bending force, blanking force, and stripper force. After completing these calculations and obtaining the total force required, the press machine's capacity is then determined to specify the appropriate press machine. The clearance value used in producing press tool components is based on a material thickness t of 1.6 mm, with an allowance value of 0.075 according to the clearance table, resulting in C=0.075×1.6=0.12. This value dictates the dimensions of the punch and die.

Piercing and blanking force calculations utilize a tensile strength of JIS G 3141 steel of 270 N/mm², resulting in $\tau_g = 0.8 \times \text{tensile strength}$, yielding τ_g = 216 N/mm². The cutting perimeters, determined using SOLIDWORKS, are: piercing 1 at 30.67 mm, piercing 2 at 9.30 mm, piercing 3 at 91.36 mm, and blanking at 58.21 mm. The cutting forces are calculated using Equation (1) resulting in forces of 10559.5 N for piercing 1, 13214.1 N for piercing 2, 31574.1 N for piercing 3, and 20117.4 N for blanking [1].

The product opening length is calculated using Equation (2) [32], with a compensation factor for the opening angle between 0° and 90°, resulting in an initial blank length of 26.89 mm [4]. The bending force is calculated using Equation (4), resulting in a force of 66997.9 N. Integrating piercing forces 1, 2, and 3, blanking force, and bending force gives a total required force of 66997.9 N, with a stripper force of 6699.79 N.

The maximum punch length is determined to be 49 mm, but a safety margin is applied with a length of 40 mm. The die thickness is set at 18.9 mm, and the minimum stripper plate thickness is determined to be

DOI: 10.36805/jtmmx.v%vi%i.7763

12.16 mm. Deflection calculations on the punch and die ensure component strength and reliability. The maximum deflections for punch piercing 1-3 are 0.02 µm, 0.07 µm, and 0.06 µm respectively, while punch blanking deflection is 0.02 µm. Deflection on the die is 0.003 µm, and on the stripper plate is 0.008 µm. Stress on punch piercing 1-3 is calculated as 129.5 N/mm², 373.8 N/mm², and 303.2 N/mm² respectively, with punch blanking stress at 71.5 N/mm².

Safety factor calculations show values ranging from 0.5 to 2.3, ensuring sufficient safety margins for operation. Specifically, safety factors for punch piercing 1, 2, 3, and blanking are 1.29, 0.5, 0.6, and 2.3 respectively. The calculation and analysis of power press tonnage requirements provide a comprehensive view of press machine design and capacity needed for material forming. This finding corroborates with Khoirudin et al.'s (2020) [33] research on piercing and bending forces, validating our analytical approach. Our results also align with Folle et al.'s (2018) [34] emphasis on safety in press machine design and echo Zhang et al.'s (2009) [35] insights on optimizing component design for performance and longevity. These comparisons underscore the reliability and relevance of our analytical method, establishing a solid foundation for press machine development in material-forming industries.

3.2. Theoretical and numerical comparation

A simulation analysis of loading was conducted to determine the maximum stress and deflection occurring in the created model press tool. This study involves simulations of the punch and die parts of the press tool using SKD 11 material according to JIS G4404 standards. This simulation process obtained values for von Mises stress and deflection. According to research reported by Ardianto et al. [10], if the von Mises stress value exceeds the yield strength of the material, then the analysis is considered unsuccessful. The research conducted by Arora. A. et al. [9] on the die section demonstrated that the design is safe. Furthermore, a comparative analysis of the developed maximum stress and stress results revealed that the developed maximum stress is very low.

The results of the comparative analysis between manual calculations and calculations using Solidworks Student Version 2018 software are presented in **Table 2**.

Table 2. The comparation of numerical analysis and theoretical analysis

No.	Descriptions	Dimension (mm)	Numerical analysis				Theoretical analysis		Yield Strength (N/mm^2)
			Deflexion (mm)		Stress (N/mm^2)		Deflexion (mm)	Stress (N/mm^2)	
			min	max	min	max			
1	Punch piercing 1	Indeterminate	0	0.03	3.7	205.6	0.02	161.9	297
2	Punch piercing 2	Indeterminate	0	0.05	0.23	439.4	0.07	373.8	297
3	Punch piercing 3	Indeterminate	0	0.06	1.8	568.5	0.06	303.2	297
4	Punch blanking	Indeterminate	0	0.02	1.4	146.8	0.02	71.5	297
5	Die	85x135x30	0	0.001	0.5	11.7	0.002	4.96	297
6	Striper plate	85X135X16	0	0.0006	0.03	1.6	0.003	0.6	297

3.3. Boundary punch piercing

The simulation conducted on punch piercings 1, 2, and 3 yielded crucial insights into their performance. For punch piercing 1, the maximum von Mises stress was recorded at 205.6 N/mm². This value, although significant, remains well below the yield strength of SKD 11 JIS G4404 material, which is 2970

DOI: 10.36805/jtmmx.v%vi%i.7763

N/mm². It indicates that punch-piercing one can withstand the applied compressive force without a significant risk of failure.

Furthermore, the deflection or displacement of punch piercing 1 measured 0.028 mm, indicating a relatively minor deformation response of the material under these operational conditions. The maximum von Mises stress node was located at point 44183 out of 46417 evaluated nodes, highlighting a concentrated stress distribution in specific areas of the punch piercing.

A simulation analysis was conducted on the research conducted by Skampardonis et al. [30] in which components were created with Ansys Workbench commercial code. The type of analysis selected was static analysis, in which each part was affixed at one end and the other end was free. The appropriate load was applied to each part at the free end. According to the Von Mises failure criteria, all parts demonstrated the capacity to withstand the applied load without failure. In the simulation setup, the oblong punch surface was fixed at one end while subjected to compressive forces at the opposite end. Figure 3 illustrates the results of von Mises stress and displacement simulations for punch piercing 1.

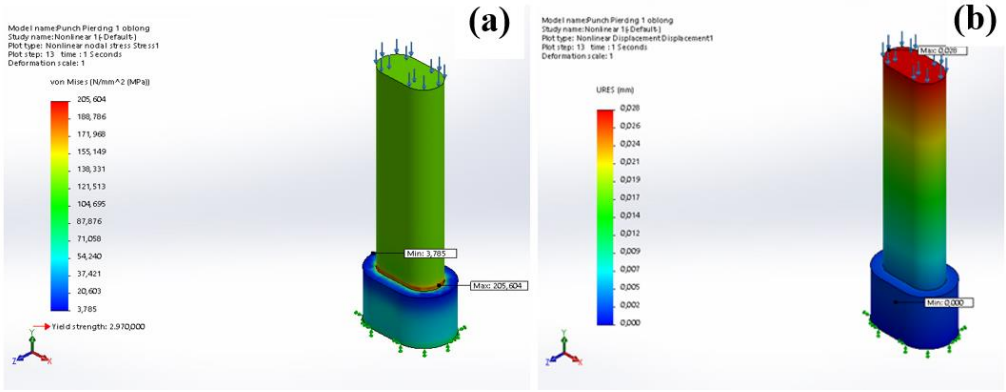

Figure 3. Boundary punch piercing 1: (a) Von Mises Stress, (b) Displacement

In the simulation of punch piercing 2, the analysis revealed a maximum von Mises stress of 439.4 N/mm², which also remains below the yield strength of SKD 11 JIS G4404 material. Additionally, the deflection was measured at 0.05 mm, indicating a controlled deformation response of the material under the applied conditions. The graphical representation of maximum von Mises stress locations highlighted stress concentrations at specific points, suggesting areas that could benefit from potential improvements or design modifications to mitigate local stress. Figure 4 depicts the results of von Mises stress and displacement simulations for punch piercing 2.

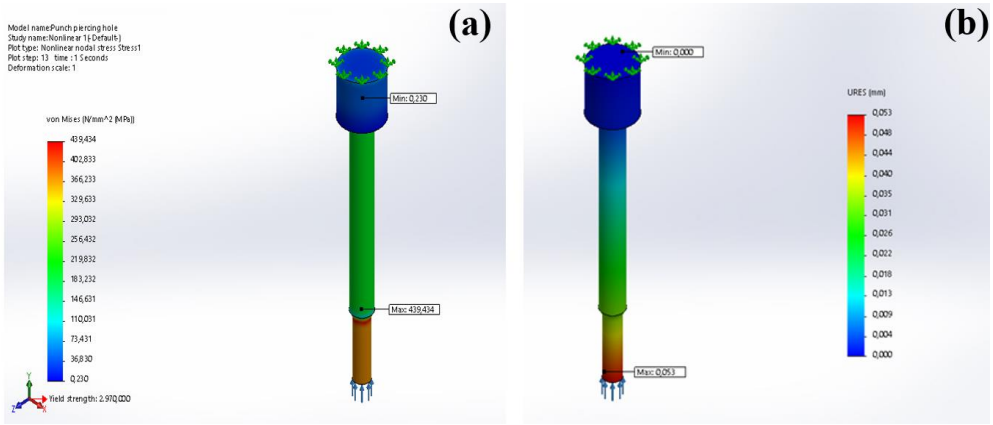

Figure 4. Boundary punch piercing 2: (a) Von Mises Stress, (b) Displacement

DOI: 10.36805/jtmmx.v%vi%i.7763

In the simulation of punch piercing 3, the analysis revealed a maximum von Mises stress of 568.5 N/mm², which also remains below the yield strength of SKD 11 JIS G4404 material. The deflection for punch piercing three was measured at 0.06 mm, indicating a slightly higher deformation response compared to the previous piercings. The graphical representation of maximum von Mises stress locations showed a similar stress distribution pattern as observed in the previous piercings, with concentrated stress points identified at specific nodes. It indicates potential areas for improvement or design adjustments to mitigate local stress concentrations. Figure 5 depicts the results of von Mises stress and displacement simulations for punch piercing 3.

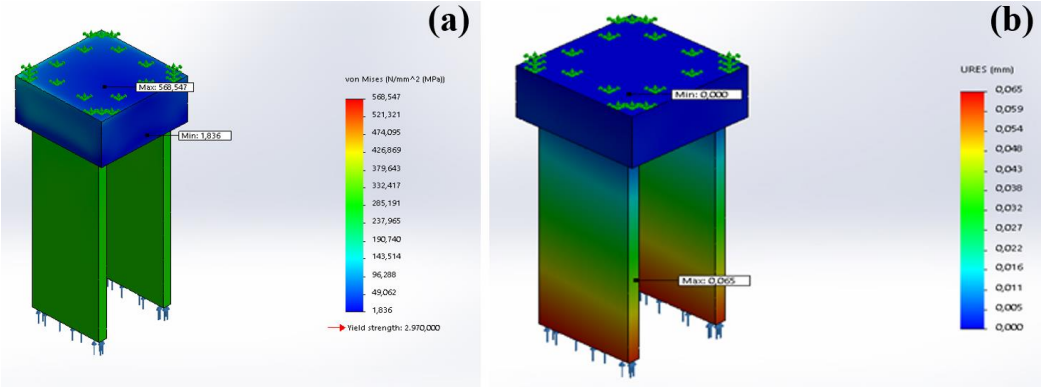

Figure 5. Boundary punch piercing 3: (a) Von Mises Stress, (b) Displacement

The simulation of punch piercing one revealed a maximum von Mises stress value of 205.6 N/mm². This value, while significant, does not exceed the yield strength of SKD 11 JIS G4404 material, which is 2970 N/mm². It indicates that with punch piercing, one can endure the applied compressive force without experiencing significant failure. Furthermore, the deflection or displacement of punch piercing one was measured at 0.028 mm, indicating a relatively minor deformation response of the material under these conditions. The maximum von Mises stress node was identified at node 44183 out of 46417 nodes evaluated, highlighting a concentrated stress distribution in a specific area of the punch piercing. In the simulation setup, the oblong punch surface was fixed at one end while subjected to compressive forces at the opposite end.

3.4. Boundary punch blanking, dies and striper plate

The simulation results for punch blanking indicate a maximum von Mises stress of 146.8 N/mm², well below the yield strength of the material used. Likewise, the deflection during punch blanking measures approximately 0.018 mm, indicating a minor deformation response. Analysis of the maximum von Mises stress locations reveals a relatively uniform stress distribution, with the highest stress point identified at node 49129 out of a total of 55535 nodes evaluated. These findings affirm that both punch piercings and punch blanking can withstand applied loads without significant failure, aligning with the material's yield strength. Localized stress points observed in each punch piercing suggest potential areas for design optimization to minimize stress concentrations and improve overall forming process performance [36]. **Figure 6** illustrates the results of von Mises stress and displacement simulations for punch piercing 3.

Simulation results from boundary dies reveal a maximum von Mises stress value of 11.7 N/mm², significantly below the yield strength of SKD 11 JIS G4404 material. This indicates that the dies can endure applied loads without significant risk of failure. Moreover, the die's deflection or displacement is merely 0.001 mm, confirming minimal material deformation under these conditions. These findings underscore the robust design and material stability of the dies, capable of withstanding pressures encountered during the

DOI: 10.36805/jtmmx.v%vi%i.7763

blanking process. **Figure 7** illustrates the results of von Mises stress and displacement simulations on the dies.

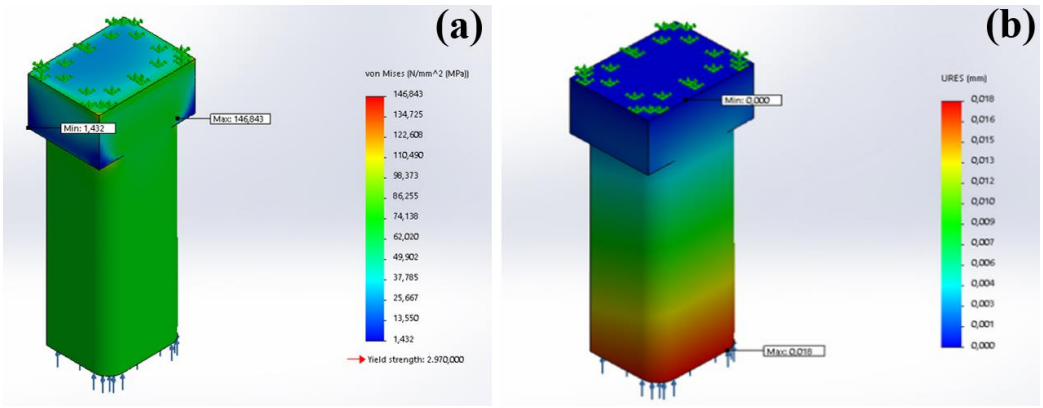

Figure 6. Boundary punch blanking 3: (a) Von Mises Stress, (b) Displacement

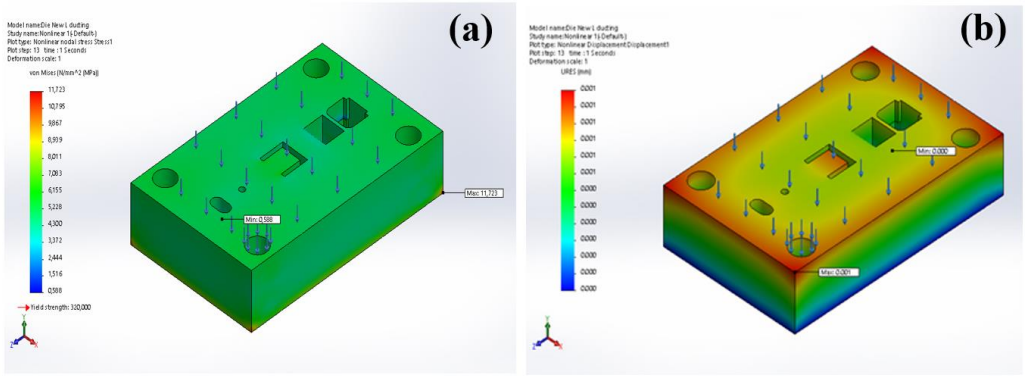

Figure 7. Boundary Dies: (a) Von Mises Stress, (b) Displacement

The stripper plate's simulation shows a maximum von Mises stress value of 1.6 N/mm², well below the yield strength of the material used. Similarly, the deflection or displacement on the stripper plate measures only 0.0006 mm, indicating minimal material deformation. It confirms the stripper plate's capability to withstand applied pressures effectively without significant deformation, thus ensuring stability and reliability in the blanking process. **Figure 8** displays the simulation results of von Mises stress and displacement on the stripper plate.

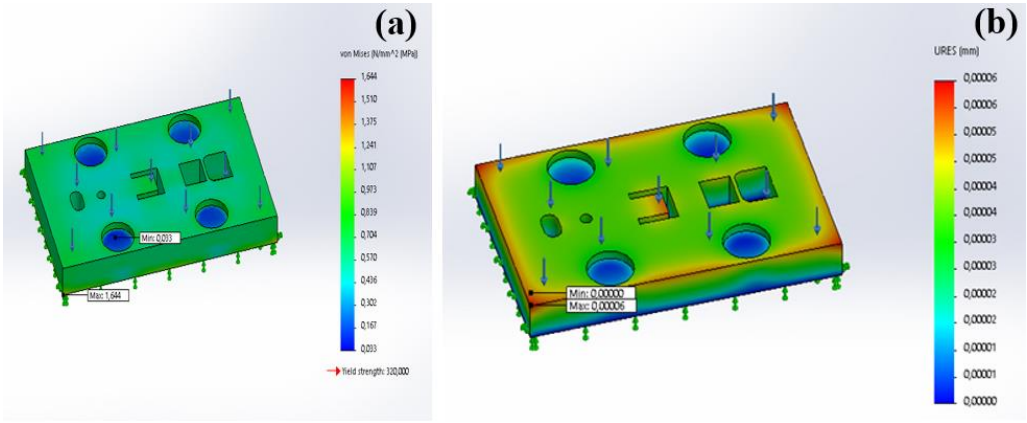

Figure 8. Boundary striper plate: (a) Von Mises Stress, (b) Displacement

DOI: 10.36805/jtmmx.v%vi%i.7763

Based on the simulation results for punch blanking, dies, and the stripper plate, it is evident that all components exhibit satisfactory performance in withstanding pressure loads and deformation responses [36]. Punch blanking shows uniform stress distribution and minimal deflection, ensuring accurate material cutting without significant deformation. The dies demonstrate robust strength and stability, with stress levels well below the material's yield strength and negligible deformation, allowing for repeated use without risk of failure [32]. Similarly, the stripper plate proves effective in withstanding pressure, showing minimal stress distribution and deformation response, thereby facilitating consistent and efficient operation in production processes. Overall, these simulation outcomes provide confidence that the blanking process using these components can be conducted safely, efficiently, and reliably to produce high-quality products.

4. Conclusion

In summary, the analysis of the power press's tonnage requirements ensures that piercing, bending, blanking, and stripping forces are carefully considered. With a required force of approximately 66,997.9 N and a press machine capacity of 8.8 tons, safety and efficiency in the manufacturing process are assured.

a. The design for the L-Hanger ducting product can be optimized into a progressive tool using precise calculations and catalog references.
b. Simulation results show maximum von Mises stress values: piercing 1 at 205.6 N/mm², piercing 2 at 439.4 N/mm², punch piercing 3 at 568.5 N/mm², punch blanking at 146.8 N/mm², dies at 11.7 N/mm², and stripper plate at 1.6 N/mm². These values are well below the yield strength of SKD 11 JIS G4404 material (2970 N/mm²).
c. Deflection values are as follows: piercing 1 at 0.028 mm, piercing 2 at 0.05 mm, punch piercing 3 at 0.06 mm, punch blanking at 0.018 mm, dies at 0.001 mm, and stripper plate at 0.006 mm. The maximum von Mises stress node is identified at node 64019 out of 64378.
d. Punch piercings 1, 2, and 3 demonstrate resilience to applied pressure loads, aligning with the yield strength of SKD 11 JIS G4404 material. Punch piercing 1, with 205.6 N/mm² stress and 0.028 mm deflection, shows controlled deformation. Punch piercings 2 and 3 exhibit higher stresses (439.4 N/mm² and 568.5 N/mm²) and slighter deflections (0.05 mm and 0.06 mm), with stress concentration at specific points suggesting areas for potential design optimization. These simulations confirm the reliability and performance of the punch piercings, ensuring efficient and consistent manufacturing processes.

The uniform stress distribution and minimal deformation on punch, die, and stripper plate validate the robustness of the analysis method and press machine design. Punch blanking, dies, and stripper plates exhibit satisfactory performance under pressure and deformation, ensuring safe and high-quality product manufacturing in the material forming industry. Overall, these results provide confidence in the effective implementation of the blanking process using these components.

.

AUTHOR'S DECLARATION

Authors' contributions and responsibilities

The authors have played crucial roles in conceiving and designing the study. They actively engaged in data analysis, interpretation, and discussions of the results. All authors have thoroughly reviewed and approved the final manuscript, underscoring their collective and individual contributions to the research endeavor.

DOI: 10.36805/jtmmx.v%vi%i.7763

Acknowledgment

The author extends heartfelt thanks to colleagues at PT Gama Satya Engineering for their valuable discussions on the design of these progressive dies. Gratitude is also extended to the supervising faculty for their guidance throughout this assignment and to the author's parents for their unwavering support and prayers. Special thanks are due to colleagues in Mechanical Engineering for their support and constructive feedback. Lastly, appreciation goes to the entire Buana Perjuangan University Karawang LAB Team for providing essential resources and a conducive environment that facilitated the completion of this assignment.

Availability of data and materials

All data from this study are accessible through the authors.

Competing interests

The authors declare no competing interest.

References

[1] I. Suchi, Handbook of Die Design 2nd Edition, 1998. [Online]. Available.

[2] S. Sukarman *et al.*, "The Square cup deep drawing: Technology transfer from experts to increase production in small and medium enterprise (SME) groups," *Mechanical Engineering for Society and Industry*, vol. 4, no. 1, pp. 38-49, 2024.

[3] Khoirudin, Sukarman, D. Mulyadi, A. Fauzi, and N. Rahdiana, "Evaluate the spring-back/spring-go phenomenon in low carbon steel sheet v-bending using an experimental method," presented at the 3rd International Conference of Bio-Based Economy for Application and Utility, 2023.

[4] N. Rahdiana, Sukarman, Khoirudin, A. Abdulah, and A. D. Shieddieque, "Spring-Back Analysis of the Vee Bending Process for High-Strength Stainless Steel," *Jurnal Teknologi*, vol. 85, no. 3, pp. 135-144, 2023.

[5] K. Khoirudin, S. Sukarman, S. Siswanto, N. Rahdiana, and A. Suhara, "Analysis of Spring-back and Spring-go on Variation of V-Dies Bending Angle Using Galvanized SGCC Steel Sheet," *Jurnal Teknik Mesin Mechanical Xplore (JTMMX)*, vol. 3, no. 1, pp. 17-25, 2022.

[6] H. S. Payal and T. R. Gupta, "Effect of Die and Punch Geometry on Spring Back in Air Bending of Electrogalvanized CR4 Steel," *International Journal of Applied Engineering Research*, vol. 12, no. 11, 2017.

[7] S. F. d. S. Yuris, "Proses Drawing Bending Dies Bracket Bolster Isuzu Traga," *Science And Engineering National Seminar 4*, vol. 4, pp. 183–192, 2019.

[8] S. d. Jumadi, "Perancangan Compound Dies untuk Proses Blanking dan Piercing Cylinder Head Gasket Tipe TVS-N54," *SINTEK J. Mesin Teknologi*, vol. 1, pp. 23-30, 2017.

[9] A. Arora, A. Pathak, A. Juneja, P. Shakkarwal, and R. Kumar, "Design & analysis of progressive die using SOLIDWORKS," *Materials Today: Proceedings*, vol. 51, pp. 956-960, 2022.

[10] W. W. R. C. Ardinto, E.Surojo, "Perancangan Progresive Dies Komponen Ring M7 Keywords : Abstract " *MEKANIKA*, vol. 11, pp. 37-40, 2012.

[11] S. Chatti, M. Hermes, A. E. Tekkaya, and M. Kleiner, "The new TSS bending process: 3D bending of profiles with arbitrary cross-sections," *CIRP Annals*, vol. 59, no. 1, pp. 315-318, 2010.

[12] M. F. Adnan, A. B. Abdullah, and Z. Samad, "Springback behavior of AA6061 with non-uniform thickness section using Taguchi Method," *The International Journal of Advanced Manufacturing Technology*, vol. 89, no. 5-8, pp. 2041-2052, 2016.

DOI: 10.36805/jtmmx.v%vi%i.7763

[13] G. M. S. Ahmed, H. Ahmed, M. V. Mohiuddin, and S. M. S. Sajid, "Experimental Evaluation of Springback in Mild Steel and its Validation Using LS-DYNA," *Procedia Materials Science,* vol. 6, pp. 1376-1385, 2014.

[14] E. H. Ouakdi, R. Louahdi, D. Khirani, and L. Tabourot, "Evaluation of springback under the effect of holding force and die radius in a stretch bending test," *Materials & Design,* vol. 35, pp. 106-112, 2012.

[15] Y. Y. E. d. K. Hamiraj, "Optimasi Pembuatan Produk Support Melalui Analisis Proses Single Tool Menjadi Progressive Hybrid Tool," *Repository.Polman-Bandung.Ac.Id,* vol. 2, pp. 1-6.

[16] A. Adelkhani, H. Ebrahimi, and M. Attar, "The experimental and numerical study of the effects of welding angle on forming multilayered sheets in U-bending operations," *Journal of Mechanical Science and Technology,* vol. 34, no. 1, pp. 239-244, 2020.

[17] A. Badrish, A. Morchhale, N. Kotkunde, and S. K. Singh, "Parameter Optimization in the Thermo-mechanical V-Bending Process to Minimize Springback of Inconel 625 Alloy," *Arabian Journal for Science and Engineering,* vol. 45, no. 7, pp. 5295-5309, 2020.

[18] M. Özdemir, H. Dilipak, and B. Bostan, "Numerically modeling spring back and spring go amounts and bending deformations of Cr-Mo alloyed sheet material," *Materialpruefung/Materials Testing,* vol. 62, no. 12, pp. 1265-1272, 2020.

[19] R. Srinivasan, D. Vasudevan, and P. Padmanabhan, "Influence of friction parameters on springback and bend force in air bending of electrogalvanised steel sheet: an experimental study," *Journal of the Brazilian Society of Mechanical Sciences and Engineering,* vol. 36, no. 2, pp. 371-376, 2013.

[20] S. Thipprakmas, "Spring-back factor applied for V-bending die design," *Journal of Advanced Mechanical Design, Systems, and Manufacturing,* vol. 14, no. 3, pp. JAMDSM0037-JAMDSM0037, 2020.

[21] S. Thipprakmas and W. Phanitwong, "Process parameter design of spring-back and spring-go in V-bending process using Taguchi technique," *Materials & Design,* vol. 32, no. 8-9, pp. 4430-4436, 2011.

[22] M. A. Wahed, A. K. Gupta, V. S. R. Gadi, S. K, S. K. Singh, and N. Kotkunde, "Parameter optimisation in V-bending process at elevated temperatures to minimise spring back in Ti-6Al-4V alloy," *Advances in Materials and Processing Technologies,* vol. 6, no. 2, pp. 350-364, 2020.

[23] H. Y. Yu, "Variation of elastic modulus during plastic deformation and its influence on springback," *Materials & Design,* vol. 30, no. 3, pp. 846-850, 2009.

[24] F. Z. J. Zhang, J. Ruan, dan K. He, "Study on springback behavior of carbon steel during single-point dieless forming based on neural network method," *IOP Conference Series: Materials Science and Engineering,* vol. 397, 2018.

[25] S. Sukarman, A. D. Shieddieque, C. Anwar, N. Rahdiana, and A. I. Ramadhan, "Optimization of Powder Coating Process Parameters in Mild Steel (Spcc-Sd) To Improve Dry Film Thickness," *Journal of Applied Engineering Science,* vol. 19, no. 2, pp. 1-9, 2021.

[26] I. B. Rahardja, N. Rahdiana, D. Mulyadi, S. Sumanto, A. I. Ramadhan, and S. Sukarman, "ANALISIS PENGARUH RADIUS BENDING PADA PROSES BENDING MENGGUNAKAN PELAT SPCC-SD TERHADAP PERUBAHAN STRUKTUR MIKRO," vol. 01, no. 01, pp. 1-10, 2020.

[27] S. Sukarman, K. Khoirudin, M. Murtalim, D. Mulyadi, and N. Rahdiana, "Evaluasi Desain Bejana Bertekanan pada Radiator Cooling System Menggunakan Material SPCC-SD," *Rekayasa: Journal of Science adn Technology,* vol. 14, no. 1, pp. 10-16, 2021.

[28] JIS G 3141, "JIS G 3141 Cold-reduced carbon steel sheets and strips," ed, 2005.
[29] *JIS G 4404 Alloy Tool Steels*, 2015.
[30] M. A. Rizza, "Analisis Proses Blanking dengan Simple Press Tool," *Jurnal Rekayasa Mesin*, vol. 5, pp. 85-90, 2014.
[31] K. Khoirudin, S. Sukarman, N. Rahdiana, and A. Fauzi, "ANALISIS FENOMENA SPRING-BACK / SPRING-GO FACTOR PADA LEMBARAN BAJA KARBON RENDAH MENGGUNAKAN PENDEKATAN EKSPERIMENTAL," *Jurnal Teknologi*, vol. 14, no. 1, 2022.
[32] I. Suchy, *Handbook of Die Design*, second ed. McGraw-Hill, 2006, pp. 327-327.
[33] K. Khoirudin *et al.*, "A Report on Metal Forming Technology Transfer from Expert to Industry for Improving Production Efficiency," *Mechanical Engineering for Society and Industry*, vol. 1, no. 2, pp. 96-103, 2021.
[34] L. F. Folle and L. Schaeffer, "Evaluation of Contact Pressure in Bending under Tension Test by a Pressure Sensitive Film," *Journal of Surface Engineered Materials and Advanced Technology*, vol. 06, no. 04, pp. 201-214, 2016.
[35] Y. Zhang and G. Cui, "Finite element simulation of springback in sheet metal bending," *Proceedings - 2009 International Conference on Information Engineering and Computer Science, ICIECS 2009*, pp. 1-4, 2009.
[36] S. Sukarman, C. Anwar, N. Rahdiana, K. Khoirudin, and A. I. Ramahdan, "ANALISIS PENGARUH RADIUS DIES TERHADAP SPRINGBACK LOGAM LEMBARAN STAINLESS-STEEL PADA PROSES BENDING HIDROLIK V-DIE," *Jurnal Teknologi*, vol. 12, no. 2, pp. 123-132, 2 July 2020 2020.

DOI: 10.36805/jtmmx.v%vi%i.7763